CANCER DIAGNOSIS & PROGNOSIS *5*: 268-279 (2025)
doi: 10.21873/cdp.10439

The Role of p300 and TMPRSS2 in Prostate Cancer: Immunohistochemical Perspectives and Gleason Correlations

CHARITOMENI GIOUKAKI[1†], ALEXANDROS GEORGIOU[1†], PANAGIOTIS SARANTIS[2], KOSTAS PALAMARIS[1], ANDREAS C. LAZARIS[1], CHRISTOS ALAMANIS[3] and GEORGIA ELENI THOMOPOULOU[4]

[1]1st Department of Pathology, School of Medicine, National and Kapodistrian University of Athens, Athens, Greece;
[2]Department of Biological Chemistry, School of Medicine, National and Kapodistrian University of Athens, Athens, Greece;
[3]1st Urology Department, Laiko Hospital, National and Kapodistrian University of Athens, Athens, Greece;
[4]Cytopathology Department, Attikon University Hospital, National and Kapodistrian University of Athens, Athens, Greece

Abstract

Background/Aim: Transmembrane protease, serine 2 (TMPRSS2), and E1A-associated protein (p300) are important factors in prostate cancer (PCa) pathogenesis, playing significant roles in androgen receptor (AR) signaling and tumor progression. Despite their established role in PCa biology, their immunohistochemical alterations across different Gleason patterns and histological grades remain unclear. This experimental study aimed to assess TMPRSS2 and p300 expression in non-malignant and cancerous prostate tissues, correlating their localization and intensity with Gleason scores and tumor aggressiveness.

Materials and Methods: A total of 58 paraffin-embedded prostate adenocarcinoma (PRAD) tissue sections from male patients who underwent radical prostatectomy, including low- and high-grade tumors and high-grade prostatic intraepithelial neoplasia (HGPIN), were analyzed. Immunohistochemistry (IHC) for TMPRSS2 and p300 was performed. Two independent pathologists conducted H-score assessments with complete interobserver concordance, evaluating staining intensity, localization, and expression patterns, correlating findings with Gleason scores and cancer stage.

Results: TMPRSS2 and p300 exhibited variable expression levels across all tissue samples. While TMPRSS2 expression increased in aggressive tumors, its staining intensity did not change significantly across different Gleason grades.

continued

†These Authors contributed equally to this work.

Andreas C. Lazaris, First Department of Pathology, Medical School, National and Kapodistrian University of Athens, 75 Mikras Asias Street, Bld 10, Goudi, 11527 Athens, Greece. Tel: +30 6972910807, e-mail: alazaris@med.uoa.gr; Charitomeni Gioukaki, First Department of Pathology, Medical School, National and Kapodistrian University of Athens, 75 Mikras Asias Street, Bld 10, Goudi, 11527 Athens, Greece. Tel: +30 6981747074, e-mail: charitomenig@med.uoa.gr

Received March 16, 2025 | Revised March 26, 2025 | Accepted March 27, 2025

p300 over-expression was significantly associated with aggressive tumors, particularly Gleason pattern 5 (p=0.011). High-grade tumors [Gleason ≥7(4+3)] demonstrated higher p300 expression compared to low-grade tumors [Gleason ≤7(3+4)], with minimal staining observed in Gleason score 6.
Conclusion: Expression patterns of TMPRSS2 and p300 correlate with PCa aggressiveness. These findings support the growing evidence suggesting their potential role as prognostic markers and therapeutic targets. The implementation of well-designed studies on a larger scale is of utmost importance, to draw safer conclusions.

Keywords: Prostate cancer, TMPRSS2, p300, molecular pathology, prognostic biomarker precision medicine.

Introduction

Prostate cancer (Pca) is the most common malignancy in men and the second leading cause of cancer-related deaths among males (1). The discovery of the molecular mechanisms underlying the pathogenesis and progression of PCa has significantly enhanced our understanding of its molecular pathology. This shift in knowledge has also transformed clinical management strategies, aligning them more closely with the principles of precision medicine (2, 3). To provide context for the present study, it is important to acknowledge our recent work, including a 2023 review, which explored the roles of transmembrane protease, serine 2 (TMPRSS2) and E1A-associated protein (p300) in PCa. In that review, we outlined their molecular mechanisms and highlighted how their expression levels correlate with PCa progression. The review also discussed the potential of these proteins as diagnostic markers and therapeutic targets, providing a solid foundation for further research in this area (4).

TMPRSS2 is a member of the type II transmembrane serine protease (TTSP) family, located on chromosome 21q22.3 (5). Its expression is elevated in prostate epithelial cells, regulated by androgens due to androgen-responsive elements in its 5'-untranslated region (UTR) regions (6).

It is also a pivotal factor in PCa's molecular pathology. The TMPRSS2:ERG fusion, frequently observed in PCa samples, correlates with reduced lymphocytic infiltration, potentially impacting the tumor's immune response, which is a known prognostic factor for survival (7-9). Over-expression of TMPRSS2 has been linked to the regulation of various hallmark malignancy traits, such as activation of epithelial-to-mesenchymal transition, which increases tumor cell invasiveness and metastasis (10), *via* activation of cell survival, and angiogenesis (11). Furthermore, recent evidence suggests that TMPRSS2:ERG gene fusions, commonly found in PCa, may have predictive value for treatment resistance. Poulsen *et al.* (12) reported that the presence of TMPRSS2:ERG fusion could indicate resistance to PARP inhibitors in metastatic castration-resistant prostate cancer (mCRPC), highlighting the broader clinical relevance of TMPRSS2 beyond tumor biology. These findings underscore the importance of investigating TMPRSS2 expression patterns not only for prognostic insight but also for potential therapeutic decision-making.

P300, a lysine acetyltransferase encoded by the *EP300* gene on chromosome 22q13.2, acts as a co-activator for transcription factors, facilitating epigenetic modifications in chromatin structure (13) and regulating various physiological processes, including DNA damage response, cell differentiation, proliferation, and apoptosis (14). Over-expression of the EP300 gene is linked to poor prognosis in various cancers, including human hepatocellular carcinoma and esophageal squamous carcinoma (15, 16).

In the context of PCa, p300 functions as a co-activator of the androgen receptor (AR), enhancing its signaling and activity (17). Elevated p300 levels have been associated with larger tumor volumes, extra prostatic extension, seminal vesicle involvement, and aggressive tumor characteristics, indicating an increased risk of biochemical

recurrence and higher Gleason scores (18). Additionally, p300 is up-regulated in docetaxel-treated patients with PCa, contributing to chemotherapy resistance and promoting metastasis (19).

Hypothesizing that the expression patterns of p300 and TMPRSS2 may be involved in the progression and aggressiveness of PCa, we investigated their immunohistochemical expression in PCa specimens and their association with key histopathological parameters, including Gleason scores and tumor stage. The purpose of this research was to explore whether p300 and TMPRSS2 can serve as prognostic or predictive markers in PCa, contributing to a more comprehensive understanding of their significance in the molecular basis of the disease. Further large-scale investigations are essential to fully elucidate their implications in PCa progression.

Materials and Methods

Patient sample collection and characterization. As part of the study, formalin-fixed paraffin-embedded (FFPE) tissues from 87 radical prostatectomy specimens were initially reviewed. Following a thorough evaluation, 32 cases were excluded from TMPRSS2 analysis and 29 cases from p300 analysis due to technical limitations and failure to meet our predefined research criteria. As a result, 55 cases were analyzed for TMPRSS2 expression, while 58 cases were assessed for p300 expression.

Low-grade PCas (Gleason grade pattern 3) accounted for 51.72% of cases, while high-grade PCas (Gleason grade patterns 4 and 5) comprised 48.28%. Most cases were Gleason score 3+4 (48.27%) and 4+3 (27.58%) (Table I).

Data from 58 male patients diagnosed with prostate adenocarcinoma (PRAD) who underwent radical prostatectomy were retrospectively obtained from the archives of the pathology laboratory within the First Department of Pathology at the School of Medicine, NKUA, "Laikon" General Hospital in Athens, Greece. The selected cases, collected between 2018 and 2022, encompassed Gleason scores ranging from 6 to 10. The patients' ages ranged from 51 to 81 years.

Table I. *Descriptive statistics of Gleason grade patterns in prostate cancer (PCa) cases.*

Number of cases (n)	Percentage %	Gleason Score	ISUP Grade
28	48.27	(3+4)	2
16	27.58	(4+3)	3
10	17.24	(4+5)	4
1	1.72	(5+4)	5
2	3.44	(3+3)	1
1	1.72	(4+4)	4
Total: 58			

ISUP: International Society of Urological Pathology.

The evaluated cases included a spectrum of PCa grades, encompassing both low-grade tumors (Gleason pattern 3) and high-grade tumors (Gleason patterns 4 and 5). For our analysis, low-grade PCa was defined as Gleason scores of 6 and 7 (3+3 and 3+4), while high-grade PCa included Gleason scores from 7 to 10 (4+3, 4+4, 4+5, 5+4, and 5+5). All selected tissue samples were archived cases, and the inclusion criteria focused on the presence and percentage of PRAD and Gleason scores, ensuring a representative sample across the spectrum of PCa aggressiveness.

Tissue processing adhered to standard histopathological protocols (20). PCa tissue samples were fixed in 10% neutral buffered formalin, embedded in paraffin, and sectioned at a thickness of 3 μm using a microtome. The prepared slides then underwent hematoxylin and eosin (H&E) staining for histopathological assessment.

Pathology reports for all cases were retrieved, and H&E-stained slides from each section were meticulously reviewed. In uncertain cases, a second slide was also selected. To ensure optimal pathological evaluation and reliable immunohistochemical analysis, the most representative section was selected for each case. The slides were thoroughly examined under light microscopy by two independent, experienced pathologists.

Cases were classified according to Gleason scores based on the standard World Health Organization (WHO) histological criteria (21), with additional assessments of key pathological parameters, including cancer staging and surgical margin status (positive or negative) (Figure 1).

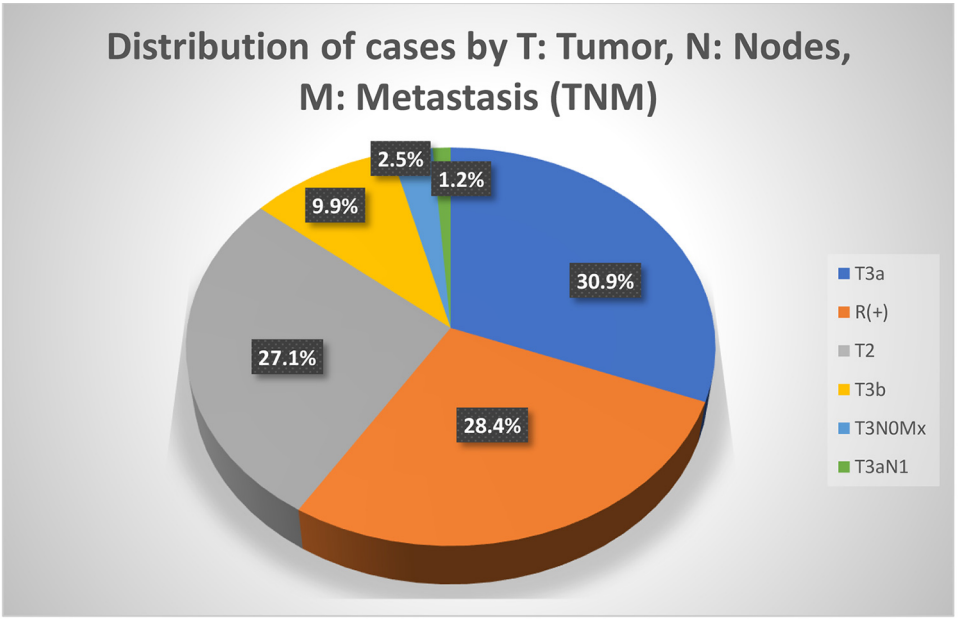

Abbreviation	Meaning
T2	Tumor confined to the prostate, detectable by DRE or imaging
T3a	Tumor has grown outside the prostate but has not spread to the seminal vesicles
T3b	Tumor has spread to the seminal vesicles
T3N0Mx	Tumor outside the prostate, N0: No lymph node involvement, Mx: Distant metastasis cannot be assessed
T3aN1	Tumor outside prostate (not in seminal vesicles), N1: Cancer has spread to regional lymph nodes
R+	Positive resection margins, indicating cancerous cells remain after surgery

Figure 1. *Distribution of cases by Tumor (T), Nodes (N), Metastasis (M) (TNM) (25).*

All procedures complied with Good Clinical Practice (GCP), Good Laboratory Practice (GLP), and health and safety regulations, as well as General Data Protection Regulation (GDPR) guidelines. The study was approved by the institutional ethical committee of Laikon General Hospital, Athens, Greece (protocol code 577/08 Sep 2022). This rigorous methodology ensured the integrity and reliability of the data collected for this study.

Immunohistochemistry. From each selected paraffin block, three new tissue sections were cut and placed on poly-L-lysine-coated slides to ensure optimal adhesion for immunohistochemical analysis. Each case included three unstained sections, with one designated for p300 analysis, one for TMPRSS2 analysis, and one reserved as a backup for potential further testing.

Immunohistochemical detection of p300 and TMPRSS2 was performed on 4-µm-thick formalin-fixed paraffin sections, which were incubated at 65˚C for 40 min prior to immunohistochemical staining. The staining procedure followed standardized protocols using the Lab Vision Autostainer 480S and the Thermo Biosystems (Waltham, MA, USA) staining protocol.

For deparaffinization, rehydration and antigen retrieval, slides were heated at 95˚C for 20 min in epredia Dewax and HIER buffer L, a low pH 6.0 citrate buffer, using

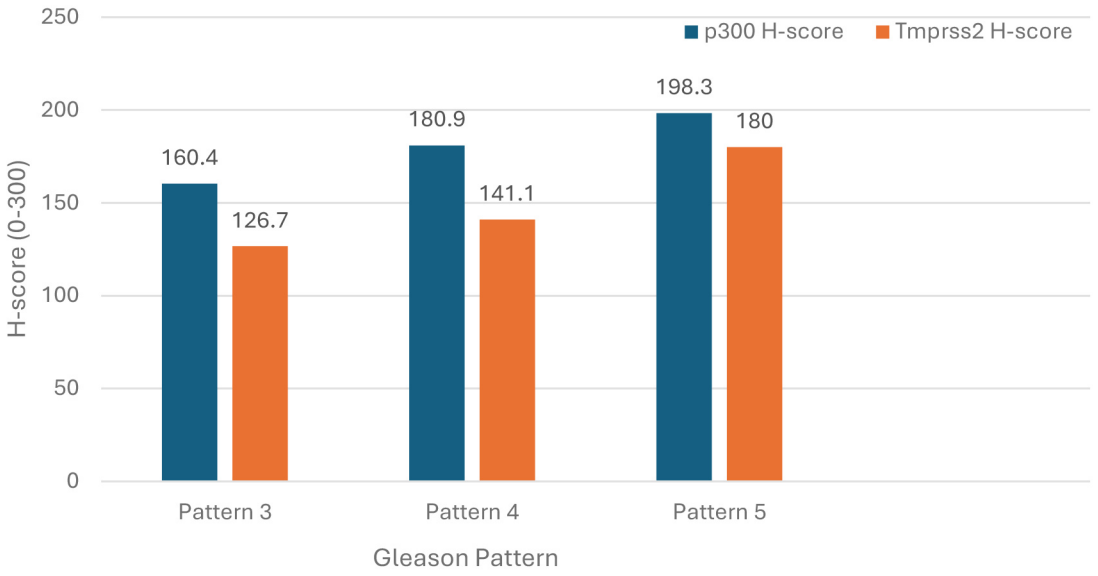

Figure 2. *Mean H-score (0-300) distribution of p300 and TMPRSS2 across different Gleason patterns.*

a microwave (Thermo PT module, 750 W, Thermo Fisher Scientific, Waltham, MA, USA). After cooling in Tris-Wash Buffer B (20X TBS) at room temperature for 15 min, the UltraVision Quanto Detection System HRP DAB (Thermo Fisher Scientific), was used for visualization. To minimize non-specific background staining, slides were pre-incubated with UltraVision Hydrogen Peroxide Block for 10 min, followed by UltraVision Protein Block for 5 min.

Primary antibody incubation was performed at 37˚C for 45 min using the following antibodies:monoclonal antibody against p300 (Clone NM-11, Mouse IgG1, diluted 1:100; Invitrogen, Waltham, MA, USA) and polyclonal antibody against TMPRSS2 (Rabbit IgG, diluted 1:50; Invitrogen).

Following incubation, slides were treated with the primary antibody amplifier Quanto (Thermo Fisher Scientific) for 10 min, followed by a 10-min application of HRP Polymer Quanto. Immunostaining was visualized using 3,3-diaminobenzidine (DAB), and Harris' hematoxylin was used for counterstaining. Coverslips were applied with permanent mounting media.

For positive controls, colon cancer tissue was used for p300, while normal human testis tissue was used for TMPRSS2. A negative control was obtained by replacing the primary antibody with normal mouse IgG. Immunohistochemical assessment was conducted using the H-score, a semi-quantitative measure of protein expression. The H-score was calculated by multiplying the staining intensity (graded 1 to 3) by the percentage of positive cells, yielding a total score ranging from 0 to 300. Nuclear and cytoplasmic staining in epithelial neoplastic cells were evaluated separately. H-score was estimated by two pathologists (A.G. and K.P.) with complete interobserver concordance.

Statistical analysis. Descriptive statistics were calculated to summarize the distribution of H-scores for TMPRSS2 and p300 across different Gleason patterns. The results are presented in Figure 2. To determine the association between H-score and Grade, a Chi-Square Test of Independence was performed. The results are presented in Table II. To assess the relationship between the expression levels of TMPRSS2 and p300, a Pearson correlation analysis was conducted using their respective H-scores. The results of this correlation analysis are presented in Table III.

Table II. C*hi-Square test results showing the association between p300 expression (H-score) and tumor grade*.*

Test	Value	df	Asymptotic significance (2-sided)	Exact significance (2-sided)	Exact significance (1-sided)
Pearson Chi-square	6.613[a]	1	0.010		
Continuity correction[b]	4.905	1	0.027		
Likelihood ratio	9.943	1	0.002		
Fisher's exact test				0.011	0.007
Linear-by-Linear association	6.499	1	0.011		
N of valid cases	58				

[a]One cell (25.0%) has an expected count less than 5. The minimum expected count is 3.60. [b]Computed only for a 2×2 table. *Low Grade includes Gleason 6 and 7 (3+3, 3+4); High Grade includes Gleason 7 to 10 (4+3, 4+4, 4+5, 5+4, 5+5).

Results

TMPRSS2 expression. TMPRSS2 expression was evident in all cancer specimens (100%). In benign prostate tissues, TMPRSS2 was predominantly localized to the luminal site of prostatic gland cells, whereas in malignant tissues, a cytoplasmic distribution was observed. This distinct shift in staining pattern in subcellular localization correlated with increasing histological aggressiveness and was more evident in high-grade areas. These findings, however, reflect general trends observed during the analysis rather than specific quantitative or qualitative measurements.

Quantitative analysis revealed an increasing trend in TMPRSS2 expression across different Gleason patterns, as illustrated in Figure 2. The mean H-score (0-300) for TMPRSS2 staining intensity (blue bars) showed a progressive elevation in higher-grade prostate cancer. Specifically, Gleason pattern 3 exhibited the lowest TMPRSS2 expression (mean H-score: 126.7), expression moderately increased in Gleason pattern 4 (mean H-score: 141.1) and peaked in Gleason pattern 5 (mean H-score: 180.0), potentially indicating an association between higher expression rate of TMPRSS2 and more aggressive, poorly differentiated tumors. However, despite this trend, intergroup variability prevented the differences from reaching statistical significance.

P300 expression. p300 immunopositivity was observed in all evaluated specimens (100%), with significant differences in staining intensity and the proportion of positive cells between non-tumorous and cancerous tissues. Prostate cancer tissues exhibited a marked increase in both staining intensity and quantitative expression, particularly in morphological subtypes associated with higher malignant potential. Notably, cribriform structures and Gleason pattern 5 tumors demonstrated the most pronounced staining pattern (p=0.011), which was interpreted either as increased intensity of immunohistostaining (3+), or as a constant moderate intensity of staining (2+) in the majority of the cellular elements that comprised them.

A progressive increase in p300 expression was observed across different Gleason patterns. The lowest expression was detected in Gleason pattern 3 (mean H-score: 160.4), indicating reduced levels in well-differentiated tumors. Expression levels increased in Gleason pattern 4 (mean H-score: 180.9) and reached their peak in Gleason pattern 5 (mean H-score: 198.3), reinforcing the association

Table III. *Pearson correlation between TMPRSS2 and p300 H-scores.*

		P300	Tmprss2
P300	Pearson correlation	1	0.314*
	Sig. (2-tailed)	-	0.019
	N	58	55
Tmprss2	Pearson correlation	0.314*	1
	Sig. (2-tailed)	0.019	-
	N	55	58

*Correlation is significant at the 0.05 level (2-tailed).

between p300 up-regulation and poorly differentiated, high-grade tumors. The distribution of p300 H-scores across different Gleason patterns is depicted in Figure 2. Statistically significant correlation was found between p300 expression and tumor grade (χ^2 test, p=0.010; Fisher's Exact Test, p=0.011), suggesting that p300 may serve as a potential biomarker for tumor aggressiveness (Table II).

Correlation between TMPRSS2 and p300. The statistical analysis presented in Table II and Table III, supports the observed correlation between p300 and TMPRSS2 expression, reinforcing their interrelated roles in AR signaling. The Pearson correlation coefficient of 0.314 (p=0.019) (Table III) confirms a moderate but statistically significant positive association, indicating that an increase in p300 expression is accompanied by an increase in TMPRSS2 expression. The Chi-Square test results (Table II) further corroborate this finding, with the Pearson Chi-Square test (χ^2=6.613, p=0.010), Likelihood Ratio test (χ^2=9.943, p=0.002), and Fisher's Exact test (p=0.011) demonstrating a significant association between the two markers. These statistical measures suggest that the relationship between TMPRSS2 and p300 is unlikely to be due to chance and instead reflects a biologically meaningful interaction. Given that both markers are involved in AR signaling, their simultaneous up-regulation suggests a heightened activation of this pathway, which plays a pivotal role in the development and progression of PCa. This finding suggests a possible mechanistic link between these two proteins in the progression of PCa and their joint involvement in aggressive tumor phenotypes.

Discussion

Regarding TMPRSS2 immunostaining, we observed a shift in its expression pattern from membranous luminal apical surface accentuation in non-malignant prostate glands, to cytoplasmic localization as PCa progresses and its biological aggressiveness increases. In benign prostate tissues, TMPRSS2 was predominantly localized to the luminal site of prostatic gland cells (Figure 3A), whereas in malignant tissues, a cytoplasmic distribution was observed (Figure 3B and C). This distinct shift in staining pattern in subcellular localization correlated with increasing histological aggressiveness and it was more evident in high-grade areas. These findings, however, reflect general trends observed during the analysis rather than specific quantitative or qualitative measurements. This observation was particularly evident in cancerous glands, including those with a Gleason score of up to 7 and where TMPRSS2 immunostaining appeared to increase (Figure 3B). In more aggressive tumors, with higher Gleason scores [7(4+3), 8, 9], TMPRSS2 expression increases and transitions from being mainly on the cell surface to being predominantly inside the cells, particularly in poorly formed and fused glands (Figure 3C). While our study did not provide specific quantitative measurements to confirm these trends, the shift in localization represents a consistent and reproducible observation.

Additionally, our research observed a progressive increase in staining intensity and overall expression levels across different Gleason patterns. While TMPRSS2 expression was lowest in Gleason pattern 3 and progressively increased in patterns 4 and 5, intergroup variability prevented these differences from reaching statistical significance. Extensive literature review indicated that our findings align with previous studies (22, 23). Chen *et al.* generated a new murine monoclonal antibody targeting TMPRSS2 with high sensitivity and specificity and conducted a comparative analysis of TMPRSS2 expression within prostate tumors and the neighboring normal parenchymal tissue. Immunohistochemical staining was carried out on paraffin–embedded human PCa tissue sections. In the unaffected tissue, TMPRSS2 was predominantly localized to the apical plasma membrane of the epithelial cells in normal prostatic glands, demonstrating membranous expression. In contrast, TMPRSS2 exhibited perimetric distribution across the entire plasma membrane in the PCa cells, with more intense expression compared to the adjacent normal prostatic parenchyma (22).

In a similar study conducted by Lucas *et al.*, the immunohistochemical localization of TMPRSS2 in

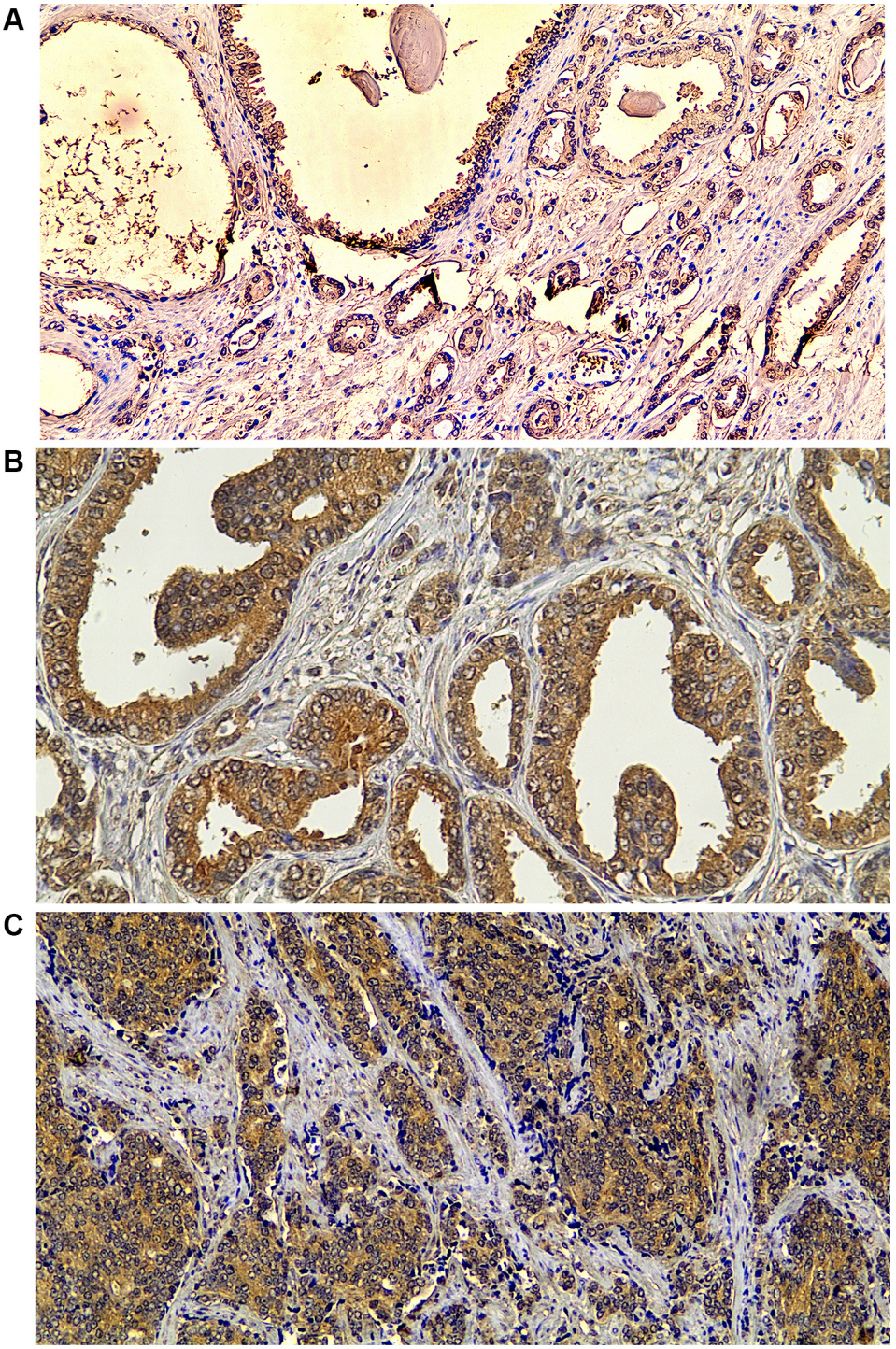

Figure 3. *Microscopic images illustrating immunohistochemical staining of transmembrane protease, serine 2 (TMPRSS2) in benign prostate tissue (A) and prostate cancer (PCa) adenocarcinoma (B, C). (A) TMPRSS2 localization in non-malignant prostate glands, predominantly observed at the luminal apical surface of epithelial cells. (B) increased protein TMPRSS2 cytoplasmic immunostaining in cancerous glands of a Gleason score 7 (3+4) adenocarcinoma. (C) shows increased expression in formations of fused glands in Gleason score 8 (4+4) adenocarcinoma. All images captured at ×100 magnification.*

prostate epithelial cells was highlighted on the luminal aspect of the plasma membrane. An additional cytoplasmic expression pattern was observed in PCa cells, particularly pronounced in Gleason pattern 3 and 4 tumors. The findings of this study also suggested that the subcellular distribution of TMPRSS2 within prostatic tissue varies across different stages of cancer progression: in normal luminal cells, predominantly membrane-only staining was observed (89%), early-stage carcinoma cells exhibited a mixed pattern of membrane and cytoplasmic staining (55% membrane, 45% cytoplasm), whereas metastatic cells primarily displayed cytoplasmic localization (13% membrane, 87% cytoplasm) (23). These findings suggest that TMPRSS2 could potentially serve as a marker for PCa aggressiveness, aiding in the assessment and prognosis of the disease.

Importantly, the expression and clinical relevance of TMPRSS2 may extend beyond its diagnostic and prognostic utility. Poulsen *et al.* (12) demonstrated that the TMPRSS2:ERG gene fusion might be associated with resistance to PARP inhibitors in mCRPC. This observation opens new avenues for therapeutic stratification, particularly in advanced disease settings. While our study focused on immunohistochemical expression rather than gene fusion status, the progressive increase in TMPRSS2 expression we observed in higher-grade tumors may reflect underlying molecular alterations such as TMPRSS2:ERG fusion, potentially linked to treatment resistance. Integrating such molecular data in future studies may help elucidate whether TMPRSS2 expression levels or fusion status could serve as predictive biomarkers for PARP inhibitor response.

Regarding p300, we noted its nuclear or peri-nuclear expression, sometimes including nuclear membrane staining. Differences were evident in the number of positive cells and the intensity of staining between non-tumorous and cancerous tissue. The intensity and quantitative expression of p300 staining were significantly elevated in morphological cancer groups known for their aggressive characteristics and higher malignant potential (Figure 4B and C). This was particularly pronounced in cribriform structures, and in cases with a Gleason pattern of 5 (p=0.011). Furthermore, p300 expression in high-grade tumors, [Gleason score ≥ 7(4+3)] was significantly higher, compared to low-grade tumors, [Gleason score ≤7(3+4)]. In contrast, in well-formed glandular structures of PRAD (Gleason score 6), we observed minimal p300 immunostaining (Figure 4A).

Our findings on p300 align with those of previous studies (18, 24). In a study of 95 patients with PCa, the immunohistochemical assessment of p300 revealed a pronounced up-regulation of p300 within neoplastic tissue in contrast to the adjacent benign parenchymal regions. Furthermore, a comprehensive analysis of the clinical data of the patient cohort and the evaluation of biopsy and prostatectomy findings demonstrated a noteworthy association between heightened p300 levels in biopsies and unfavorable clinicopathological parameters, including more advanced disease staging and PCa progression after surgery as well as a positive trend in the correlation between p300 expression levels and higher Gleason scores (17). Similar findings were observed in the research conducted by Isharwal *et al.*; p300 expression levels were notably elevated in high-grade tumors and they were also correlated with nuclear aberrations within tumor cells. Additionally, p300 levels demonstrated a prognostic value in predicting long-term biochemical recurrence-free survival in PCa (24).

High stain intensity and over-expression of p300 in higher Gleason scores were strongly associated with aggressive tumor phenotypes in PCa. This correlation underscores the pivotal role of p300 in the pathogenesis and progression of more malignant and advanced forms of PCa. Consequently, p300 could serve as a valuable prognostic marker, providing insights into likely clinical outcomes and helping to stratify patients based on their risk profiles. Moreover, the significant association between p300 over-expression and poor prognostic indicators positions it as a potential therapeutic target. By developing strategies to modulate p300 activity, it may be possible to curb tumor growth and improve patient outcomes, making p300 a focal point in the ongoing quest for more effective

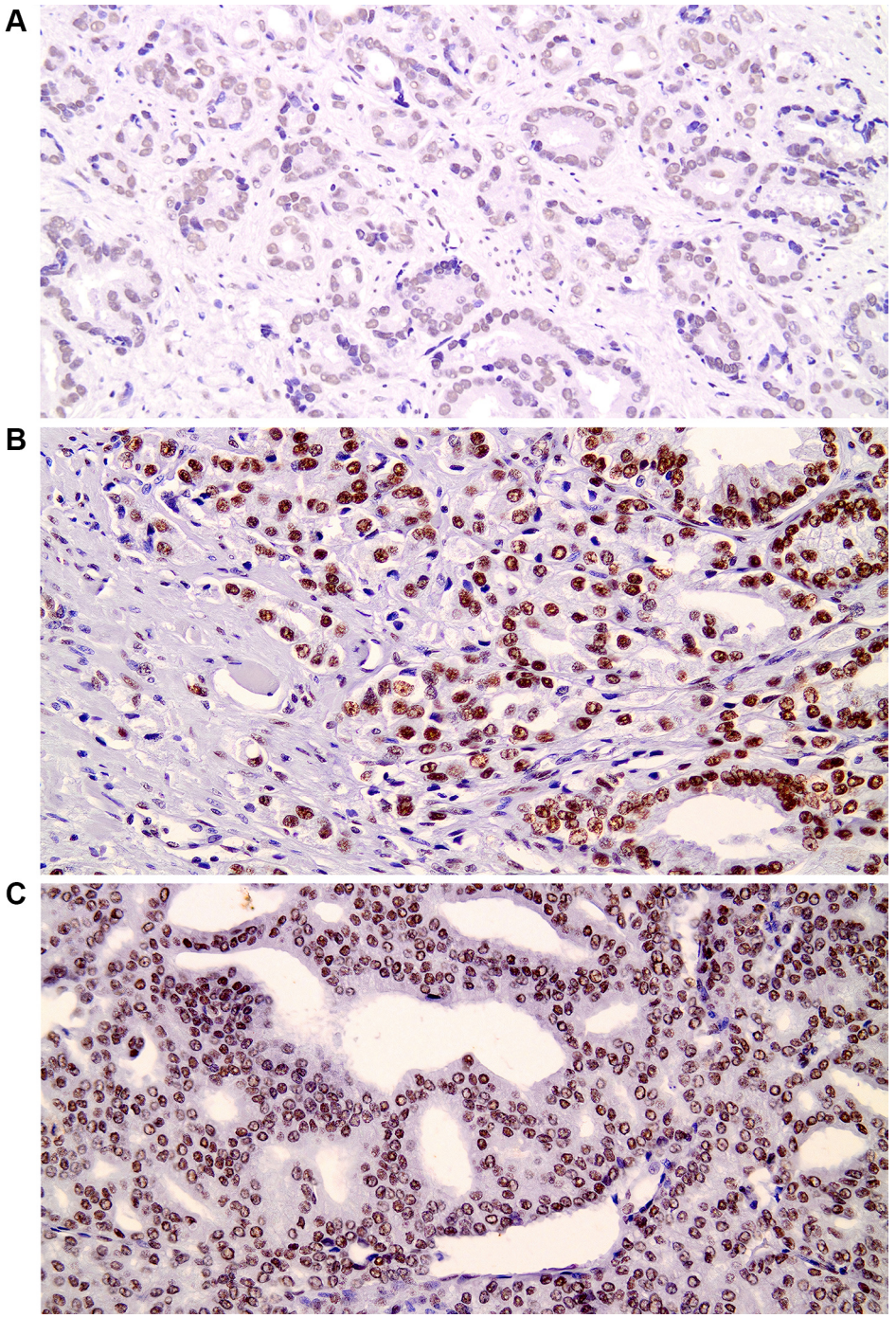

Figure 4. *Microscopic images of prostate cancer (PCa) adenocarcinoma displaying increased immunohistochemical staining for E1A-associated protein (p300) protein. Microscopic images of PCa tissue sections illustrating the progressive increase in P300 protein staining. (A) Well-formed cancerous glands (Gleason 3+3) exhibit low P300 expression, with nuclear staining of minimum intensity (1+). (B+C) Moderately and poorly differentiated carcinoma shows increased P300 staining. (B) Increased P300 immunostaining of strong intensity (3+) in poorly formed glandular elements (Gleason 4+3) adenocarcinoma. (C) Increased P300 immunoreactivity of intermediate intensity in cribriform structure and fused cancerous glands (Gleason 4+4) adenocarcinoma. All images captured at ×100 magnification.*

PCa therapies. The results of our study demonstrate a significant association between immunohistochemical H-score and Tumor Grade in the context of p300 staining.

The immunoexpression of the two markers was found to be closely interrelated; specifically, an increase in p300 expression corresponded with an increase in TMPRSS2 expression (p=0.019) (Table III). This is particularly significant given that both markers are part of the same AR pathway. This correlation is crucial in the development and progression of PCa, as it suggests a heightened activation of the AR pathway. p300, a transcriptional coactivator, may enhance AR-mediated transcription, while TMPRSS2, often involved in gene fusions like TMPRSS2-ERG, can drive oncogenic processes. Their simultaneous up-regulation indicates robust AR pathway activation, a hallmark of aggressive PCa.

Understanding the interplay between p300 and TMPRSS2 provides deeper mechanistic insights into how AR signaling promotes tumorigenesis. p300 can acetylate the AR, enhancing its activity, whereas TMPRSS2 expression, regulated by AR, can facilitate gene fusions that contribute to cancer progression. This relationship underscores the collaborative roles of p300 and TMPRSS2 in facilitating AR-driven oncogenic transcriptional programs.

Conclusion

In conclusion, the combined increase in p300 and TMPRSS2 expression levels could serve as a powerful prognostic marker. Their interrelated expression may indicate a more aggressive tumor phenotype and poorer prognosis, aiding in the stratification of patients for more tailored therapeutic approaches. Given their roles in the AR pathway, both p300 and TMPRSS2 can be considered as attractive therapeutic targets. Inhibiting p300 could disrupt AR signaling and reduce TMPRSS2 expression, potentially mitigating the oncogenic effects mediated by this pathway. This dual targeting approach could lead to the development of more effective treatment strategies, particularly for patients with AR-driven PCa.

The interrelationship between p300 and TMPRSS2 suggests they could be part of a biomarker panel for monitoring AR pathway activation. This could help in early diagnosis, assessing disease progression, and evaluating treatment responses, enhancing clinical management of PCa. In summary, the correlation between p300 and TMPRSS2 expression underscores their critical roles in the AR pathway, providing valuable insights into PCa pathogenesis, prognosis, and potential therapeutic interventions.

Conflicts of Interest

The Authors declare no conflicts of interest in relation to this study.

Authors' Contributions

A.C.L. and G.E.T. conceived the research concept for this article. C.G. conducted the experimental work. C.G. and A.G. jointly designed the article content and contributed equally to writing the manuscript. P.S. provided the statistical analysis. A.G., K.P., and assessed the H-score for each sample. C.G. and K.P. contributed to manuscript revisions. All Authors have reviewed and approved the final version of the manuscript.

Acknowledgements

Not applicable.

Funding

This research received no external funding.

References

1 Siegel RL, Miller KD, Fuchs HE, Jemal A: Cancer statistics, 2022. CA Cancer J Clin 72(1): 7-33, 2022. DOI: 10.3322/caac.21708

2 Rodrigues DN, Butler LM, Estelles DL, de Bono JS: Molecular pathology and prostate cancer therapeutics: from biology to bedside. J Pathol 232(2): 178-184, 2014. DOI: 10.1002/path.4272

3 Vlajnic T, Bubendorf L: Molecular pathology of prostate cancer: a practical approach. Pathology 53(1): 36-43, 2021. DOI: 10.1016/j.pathol.2020.10.003
4 Gioukaki C, Georgiou A, Gkaralea LE, Kroupis C, Lazaris AC, Alamanis C, Thomopoulou GE: Unravelling the role of P300 and TMPRSS2 in prostate cancer: a literature review. Int J Mol Sci 24(14): 11299, 2023. DOI: 10.3390/ijms241411299
5 Thunders M, Delahunt B: Gene of the month: *TMPRSS2* (transmembrane serine protease 2). J Clin Pathol 73(12): 773-776, 2020. DOI: 10.1136/jclinpath-2020-206987
6 Epstein RJ: The secret identities of TMPRSS2: Fertility factor, virus trafficker, inflammation moderator, prostate protector and tumor suppressor. Tumor Biol 43(1): 159-176, 2021. DOI: 10.3233/TUB-211502
7 Zhang SC, Hu ZQ, Long JH, Zhu GM, Wang Y, Jia Y, Zhou J, Ouyang Y, Zeng Z: Clinical IMPLICATIONS OF TUMOR-INFILTRATING IMMUNE CELLS IN BREAST CANCER. J Cancer 10(24): 6175-6184, 2019. DOI: 10.7150/jca.35901
8 Rao SR, Alham NK, Upton E, McIntyre S, Bryant RJ, Cerundolo L, Bowes E, Jones S, Browne M, Mills I, Lamb A, Tomlinson I, Wedge D, Browning L, Sirinukunwattana K, Palles C, Hamdy FC, Rittscher J, Verrill C: Detailed molecular and immune marker profiling of archival prostate cancer samples reveals an inverse association between TMPRSS2:ERG fusion status and immune cell infiltration. J Mol Diagnost 22(5): 652-669, 2020. DOI: 10.1016/j.jmoldx.2020.02.012
9 Zuo S, Wei M, Wang S, Dong J, Wei J: Pan-Cancer analysis of immune cell infiltration identifies a prognostic immune-cell characteristic score (ICCS) in lung adenocarcinoma. Front Immunol 11: 1218, 2020. DOI: 10.3389/fimmu.2020.01218
10 Ko CJ, Hsu TW, Wu SR, Lan SW, Hsiao TF, Lin HY, Lin HH, Tu HF, Lee CF, Huang CC, Chen MM, Hsiao PW, Huang HP, Lee MS: Inhibition of TMPRSS2 by HAI-2 reduces prostate cancer cell invasion and metastasis. Oncogene 39(37): 5950-5963, 2020. DOI: 10.1038/s41388-020-01413-w
11 Zhou F, Gao S, Han D, Han W, Chen S, Patalano S, Macoska JA, He HH, Cai C: TMPRSS2-ERG activates NO-cGMP signaling in prostate cancer cells. Oncogene 38(22): 4397-4411, 2019. DOI: 10.1038/s41388-019-0730-9
12 Poulsen TS, Lørup AN, Kongsted P, Eefsen RL, Højgaard M, Høgdall EV: *TMPRSS2:ERG* gene fusion might predict resistance to PARP inhibitors in metastatic castration-resistant prostate cancer. Anticancer Res 44(10): 4203-4211, 2024. DOI: 10.21873/anticanres.17250
13 Shiama N: The p300/CBP family: integrating signals with transcription factors and chromatin. Trends Cell Biol 7(6): 230-236, 1997. DOI: 10.1016/S0962-8924(97)01048-9
14 Goodman RH, Smolik S: CBP/p300 in cell growth, transformation, and development. Genes Dev 14(13): 1553-1577, 2000. DOI: 10.1101/gad.14.13.1553
15 Bi Y, Kong P, Zhang L, Cui H, Xu X, Chang F, Yan T, Li J, Cheng C, Song B, Niu X, Liu X, Liu X, Xu E, Hu X, Qian Y, Wang F, Li H, Ma Y, Yang J, Liu Y, Zhai Y, Wang Y, Zhang Y, Liu H, Liu J, Wang J, Cui Y, Cheng X: EP300 as an oncogene correlates with poor prognosis in esophageal squamous carcinoma. J Cancer 10(22): 5413-5426, 2019. DOI: 10.7150/jca.34261
16 Tsang FH, Law CT, Tang TC, Cheng CL, Chin DW, Tam WV, Wei L, Wong CC, Ng IO, Wong CM: Aberrant super-enhancer landscape in human hepatocellular carcinoma. Hepatology 69(6): 2502-2517, 2019. DOI: 10.1002/hep.30544
17 Welti J, Sharp A, Brooks N, Yuan W, McNair C, Chand SN, Pal A, Figueiredo I, Riisnaes R, Gurel B, Rekowski J, Bogdan D, West W, Young B, Raja M, Prosser A, Lane J, Thomson S, Worthington J, Onions S, Shannon J, Paoletta S, Brown R, Smyth D, Harbottle GW, Gil VS, Miranda S, Crespo M, Ferreira A, Pereira R, Tunariu N, Carreira S, Neeb AJ, Ning J, Swain A, Taddei D, SU2C/PCF International Prostate Cancer Dream Team, Schiewer MJ, Knudsen KE, Pegg N, de Bono JS: Targeting the p300/CBP axis in lethal prostate cancer. Cancer Discov 11(5): 1118-1137, 2021. DOI: 10.1158/2159-8290.CD-20-0751
18 Heemers HV, Debes JD, Tindall DJ: The role of the transcriptional coactivator p300 in prostate cancer progression. Adv Exp Med Biol 617: 535-540, 2008. DOI: 10.1007/978-0-387-69080-3_54
19 Gruber M, Ferrone L, Puhr M, Santer FR, Furlan T, Eder IE, Sampson N, Schäfer G, Handle F, Culig Z: p300 is upregulated by docetaxel and is a target in chemoresistant prostate cancer. Endocr Relat Cancer 27(3): 187-198, 2020. DOI: 10.1530/ERC-19-0488
20 Wolfe D: Bancroft's theory and practice of histological techniques. In: Bancroft's theory and practice of histological techniques. 8th ed. Suvarna SK, Layton C, Bancroft JD (eds.). Elsevier, pp. 73-83, 2019.
21 Humphrey PA, Moch H, Cubilla AL, Ulbright TM, Reuter VE: The 2016 WHO Classification of Tumours of the urinary system and male genital organs—Part B: Prostate and bladder tumours. Eur Urol 70(1): 106-119, 2016. DOI: 10.1016/j.eururo.2016.02.028
22 Lucas JM, True L, Hawley S, Matsumura M, Morrissey C, Vessella R, Nelson PS: The androgen-regulated type II serine protease TMPRSS2 is differentially expressed and mislocalized in prostate adenocarcinoma. J Pathol 215(2): 118-125, 2008. DOI: 10.1002/path.2330
23 Chen YW, Lee MS, Lucht A, Chou FP, Huang W, Havighurst TC, Kim K, Wang JK, Antalis TM, Johnson MD, Lin CY: TMPRSS2, a serine protease expressed in the prostate on the apical surface of luminal epithelial cells and released into semen in prostasomes, is misregulated in prostate cancer cells. Am J Pathol 176(6): 2986-2996, 2010. DOI: 10.2353/ajpath.2010.090665
24 Isharwal S, Miller MC, Marlow C, Makarov DV, Partin AW, Veltri RW: p300 (histone acetyltransferase) biomarker predicts prostate cancer biochemical recurrence and correlates with changes in epithelia nuclear size and shape. Prostate 68(10): 1097-1104, 2008. DOI: 10.1002/pros.20772
25 Rosen RD, Sapra A: TNM Classification. Treasure Island, FL, USA, StatPearls Publishing, 2025.